Simulation of Real-time Bit Error Rate in Low Earth Orbit (LEO) Satellites Narrow-band and Wide-band Telemetry Radio Link

Somaye Pirzadi
Department of Electrical Engineering, College of Electrical Engineering, Ghasr -E-Shirin Branch, Islamic Azad University, Ghasr-E-Shirin, Kermanshah, Iran
somaye.pirzadi@gmail.com

***Abstract*—While the Low Earth Orbit satellite has been placed on the determined orbit, ground station has required making a contact with satellite to receive information and control its subsystems. The time variant behavior of the satellite – station radio link should be considered in an appropriate model. This issue has been important because of its high impact on choice the type of the modulation, channel access method designing and error control. In this article the probability of error's range changes would be estimated momentarily. To achieve this purpose, at first instantaneous communication angles have been measured on the satellite theoretically, and based on these communication angles, the momentary gain in transmitter antennas would be determined. Then, the variation of the signal-to-noise rate (SNR) have been achieved momentarily and based on it, Bit error rate (BER) changes would be achieved momentarily, during the time which the LEO satellite has been in the direct view of the telemetry receiver antenna. Channels studied in this paper have been wide-band channels which have been used in transferring images and multimedia messages and these channels have been modeled due to the effects of multipath and shadowing conditions.**

***Index Terms*—Bit Error Rate, Fading channel, LEO Satellites, Radio link, Wideband Telemetry.**

I. INTRODUCTION

At the time of receiving data from flying objects or LEO satellites, shadows falling on the satellite signal cause signal attenuation. By reducing the angle between the transmitted beam and reception spot (elevation angle), the shadow zone would be widen. In this case, due to the lack of direct vision component by obstacles in the channel, multi-streaming attenuation would occur. The signal is appeared as a large number of reflecting components which have reached to the receiver after successive and multiple reflections. According to difference among random path of diffusion paths, these random components could reinforce or undermine each other. On the other hand for all systems, communicative channel between the satellite and the ground-station has been the most sensitive part of the system and limited the performance of the whole system. Therefore, providing an appropriate model for the channel is significantly required.

In a high performance model, the time variant behavior of the satellite–ground station radio link should be considered. Because this issue has performs an important role in choosing the type of modulation method, channel access method designing and error control. Considering time limitations in accessing LEO satellite or flying object, the author in this research has applied a method to calculate the error rate in LEO satellite radio links momentarily in order to reduce it in the case of any increase in the error. The mathematical equations in calculating flying objects communicative angles have been proposed by Marzban and Mohammed Pour in [1]. Based on these equations the communicative angles and SNR are calculated momentarily and then the channel is simulated. Channel models are usually classified into two categories; narrowband and wideband. Narrowband channels, for situations where the signal bandwidth is much less than coherent bandwidth in multi-path fading processes, are useful. Rayleigh channels used for the urban cellular channels, Rice channels used in the satellite mobile channels and narrowband channels useful for the aerospace telemetry are as examples for fading narrowband channel models.

In this research the channel is supposed as a wide band channel and as it is known, the main solution for the modeling effects of wideband channel is observing the channel impulse response. So far, several models have been proposed based on defined appropriate distributions for the components of channel impulse response. Choosing distribution related to each model, selecting path Taps for efficient modeling are based on measuring and statistical analysis of the measured data. Some famous models have been proposed such as; DRL model presented by German Aerospace Center [2], CCSR-ESTEC model presented by European Space Research and Technology Centre (ESTEC) [3], Saunders model et al. [4] and Rice model et al. [5].

Recently, non-stationary satellite systems with respect to the earth like LEO satellite systems have been considered. Satellite systems could be used to enhance the availability of services in the telecommunication networks. Of course, the main difference between the satellite and ground-based systems has been their transmission channel. So to improve existing systems, it has been necessary to simulate the behavior of distribution path. In this study, link would simulate to use it in telemetry station to sending command for controlling subsystems or receiving data from satellite. Also, due to the increasing rate of the users to send video and data

with high volume, controlling the status of the radio link in the channel has been needed. Generally, the channel of these systems was wideband; that is why the subject of this research has been considered.

II. CALCULATING COMMUNICATIVE ANGLES

The following algorithm was purposed to calculate the communicative angles between a transmit antenna on the satellite and a receive antenna in the ground station.

The satellite orbit parameters such as: 3-D coordinate, yaw, pitch and roll angles was obtained from simulation software (like STSPLUS software).

Cartesian coordinates of the satellite position and the receive antenna position was calculated from geographical coordinates [6, 7].

$$\begin{aligned} x_{sp} &= (M_{sp} + H_{SP}) \cdot \cos B_{sp} \cdot \cos L_{sp} \\ y_{sp} &= (M_{sp} + H_{SP}) \cdot \cos B_{sp} \cdot \sin L_{sp} \\ z_{sp} &= [M_{sp} \cdot (1 - e^2) + H_{SP}] \cdot \sin L_{sp} \end{aligned} \quad (1)$$

where; B_{sp} is latitude, L_{sp} is longitude of the satellite starting point (the first point that the satellite is seen), H_{sp} represents the height above sea level, e^2=0.00669 is Earth's eccentricity constant and M_{sp} is obtained by (2).

$$M_{sp} = \frac{6378245}{\sqrt{1 - (e^2 \sin^2 B_{sp})}} \quad (2)$$

and;

$$\begin{aligned} x_{ap} &= (M_{ap} + H_{aP}) \cdot \cos B_{ap} \cdot \cos L_{ap} \\ y_{ap} &= (M_{ap} + H_{aP}) \cdot \cos B_{ap} \cdot \sin L_{ap} \\ z_{ap} &= [M_{ap} \cdot (1 - e^2) + H_{aP}] \cdot \sin L_{ap} \end{aligned} \quad (3)$$

where; B_{ap} is latitude, L_{ap} is longitude of receiver antenna position at ground station, and H_{ap} represents the height above sea level, and M_{ap} is derived by (4).

$$M_{ap} = \frac{6378245}{\sqrt{1 - (e^2 \sin^2 B_{ap})}} \quad (4)$$

Transfer matrices M_1, M_2, M_3 mentioned in [1] are utilized to calculate the communicative angles.

Instantaneous satellite coordinates are transferred to the starting point (SP) of being seen satellite coordinate system by (5).

$$\begin{bmatrix} x_i \\ y_i \\ z_i \end{bmatrix} = \begin{bmatrix} x_{sp} \\ y_{sp} \\ z_{sp} \end{bmatrix} + M_1^T \cdot \begin{bmatrix} x_{ci} \\ y_{ci} \\ z_{ci} \end{bmatrix} \quad (5)$$

In (5), x_i, y_i, z_i are the instantaneous coordinates of path in the SP system. By matrix M_1, satellite coordinate system is transferred to the coordinate system that placed at the SP. x_{ci}, y_{ci}, z_{ci} are instantaneous coordinates of satellite's flight path, which is obtained from the simulation results at the STSPLUS environment.

$$M_1 = \begin{bmatrix} \omega_{11} & \omega_{12} & \omega_{13} \\ \omega_{21} & \omega_{22} & \omega_{23} \\ \omega_{31} & \omega_{32} & \omega_{33} \end{bmatrix} \quad (6)$$

Transfer matrix elements are obtained from the following equations:

$$\omega_{11} = -\sin B_{sp} \cdot \cos L_{sp} \cdot \cos A_{sp} - \sin L_{sp} \cdot \sin A_{sp}$$

$$\omega_{12} = -\sin B_{sp} \cdot \sin L_{sp} \cdot \cos A_{sp} + \cos L_{sp} \cdot \sin A_{sp}$$

$$\omega_{13} = \cos B_{sp} \cdot \cos A_{sp}$$

$$\omega_{21} = \sin B_{sp} \cdot \cos L_{sp} \cdot \sin A_{sp} - \sin L_{sp} \cdot \cos A_{sp}$$

$$\omega_{22} = \sin B_{sp} \cdot \sin L_{sp} \cdot \sin A_{sp} + \cos L_{sp} \cdot \cos A_{sp}$$

$$\omega_{23} = -\cos B_{sp} \cdot \sin A_{sp}$$

$$\omega_{31} = \cos B_{sp} \cdot \cos L_{sp}$$

$$\omega_{32} = \cos B_{sp} \cdot \sin L_{sp}$$

$$\omega_{33} = \sin B_{sp}$$

Equation (7) is utilized to instantaneous transfer the satellite coordinates (obtained from (5)), to the coordinates of telemetry receiver antenna.

$$\begin{bmatrix} x_{ui} \\ y_{ui} \\ z_{ui} \end{bmatrix} = M_2 \cdot \begin{bmatrix} x_i - x_{ap} \\ y_i - y_{ap} \\ z_i - z_{ap} \end{bmatrix} \quad (7)$$

Where, x_{ui}, y_{ui}, z_{ui} are the coordinates of the satellite, which this system has been transferred to antenna location system by transfer matrix defined as follows;

$$M2 = \begin{bmatrix} \gamma_{11} & \gamma_{12} & \gamma_{13} \\ \gamma_{21} & \gamma_{22} & \gamma_{23} \\ \gamma_{31} & \gamma_{32} & \gamma_{33} \end{bmatrix} \quad (8)$$

Transfer matrix elements are obtained from the following equations;

$$\gamma_{11} = -\sin B_{ap} \cdot \cos L_{ap}$$

$$\gamma_{12} = -\sin B_{ap} \cdot \sin L_{ap}$$

$$\gamma_{13} = \cos B_{ap}$$

$$\gamma_{21} = \cos B_{ap} \cdot \cos L_{ap}$$

$$\gamma_{22} = \cos B_{ap} \cdot \sin L_{ap}$$

$$\gamma_{23} = \sin B_{ap}$$

$$\gamma_{31} = -\sin L_{ap}$$

$$\gamma_{32} = \cos L_{ap}$$

$$\gamma_{33} = 0$$

Using calculated coordinates, which obtained from (7), distance between receiver antenna and satellite, receiver's antenna vertical angle and antenna's horizontal angle respectively could be obtained from (9), (10) and (11).

Distance between receiver antenna and satellite at the moment t_i is obtained as follows;

$$R_i = \sqrt{x_{ui}^2 + y_{ui}^2 + z_{ui}^2} \tag{9}$$

Antenna Elevation angle at the moment t_i is obtained as follows;

$$\beta_i = \left[\frac{y_{ui}}{\sqrt{x_{ui}^2 + z_{ui}^2}}\right] \cdot \frac{180}{\pi} \tag{10}$$

Antenna Azimuth angle at the moment t_i is obtained as follows:

$$\alpha_i = \arctan\left[\frac{z_{ui}}{x_{ui}}\right] \cdot \frac{180}{\pi} \tag{11}$$

The angle θ_i (depicted in the Fig. 1) on the satellite at the moment t_i can be calculated as follows;

$$\theta_i = \arccos\left(\frac{n_{X_{api}} \cdot x_{ui} + n_{Y_{api}} \cdot y_{ui} + n_{Z_{api}} \cdot z_{ui}}{\sqrt{(x_{ui}^2 + y_{ui}^2 + z_{ui}^2)(n_{X_{api}}^2 + n_{Y_{api}}^2 + n_{Z_{api}}^2)}}\right) \cdot \frac{180}{\pi} \tag{12}$$

In which, $n_{X_{api}}$, $n_{Y_{api}}$, $n_{Z_{api}}$ are obtained as follows;

$$\begin{bmatrix} n_{X_{api}} \\ n_{Y_{api}} \\ n_{Z_{api}} \end{bmatrix} = M_2 \cdot M_1^T \begin{bmatrix} n_{X_{Ci}} \\ n_{Y_{Ci}} \\ n_{Z_{Ci}} \end{bmatrix} \tag{13}$$

$$\begin{bmatrix} n_{X_{Ci}} \\ n_{Y_{Ci}} \\ n_{Z_{Ci}} \end{bmatrix} = M_3^T \begin{bmatrix} 1 \\ 0 \\ 0 \end{bmatrix} \tag{14}$$

In which, M_3 is converter matrix for coordinate system, and can be defined by (15).

$$M_3 = \begin{bmatrix} \delta_{11i} & \delta_{12i} & \delta_{13i} \\ \delta_{21i} & \delta_{22i} & \delta_{23i} \\ \delta_{31i} & \delta_{32i} & \delta_{33i} \end{bmatrix} \tag{15}$$

Transfer matrix elements are obtained from the following equations;

$$\delta_{11i} = \cos\vartheta_i \cdot \cos\psi_i$$

$$\delta_{12i} = \cos\gamma_i \cdot \sin\psi_i + \sin\gamma_i \cdot \sin\vartheta_i \cdot \cos\psi_i$$

$$\delta_{13i} = \sin\gamma_i \cdot \sin\psi_i - \cos\gamma_i \cdot \sin\vartheta_i \cdot \cos\psi_i$$

$$\delta_{21i} = -\cos\vartheta_i \cdot \sin\psi_i$$

$$\delta_{22i} = \cos\gamma_i \cdot \cos\psi_i - \sin\gamma_i \cdot \sin\vartheta_i \cdot \sin\psi_i$$

$$\delta_{22i} = \sin\gamma_i \cdot \cos\psi_i + \cos\gamma_i \cdot \sin\vartheta_i \cdot \sin\psi_i$$

$$\delta_{31i} = \sin\vartheta_i$$

$$\delta_{32i} = -\sin\gamma_i \cdot \cos\vartheta_i$$

$$\delta_{33i} = \cos\gamma_i \cdot \cos\vartheta_i$$

Where;

$\vartheta = Pitch,\ \gamma = Roll,\ \psi = Yaw$

The angle φ_i (depicted in the Fig. 1) on the satellite at the moment t_i can be calculated as follows;

$$\varphi_i = \arctan\left[\frac{y'_{ui}}{z'_{ui}}\right] \cdot \frac{180}{\pi} \tag{16}$$

Where;

y'_{ui} and z'_{ui} is obtained from (17) and (18).

$$\begin{bmatrix} x'_{ui} \\ y'_{ui} \\ z'_{ui} \end{bmatrix} = M_3^T \begin{bmatrix} x_u - x_{ci} \\ y_u - y_{ci} \\ z_u - z_{ci} \end{bmatrix} \tag{17}$$

$$\begin{bmatrix} x_u \\ y_u \\ z_u \end{bmatrix} = M_1 \begin{bmatrix} x_{ap} - x_{sp} \\ y_{ap} - y_{sp} \\ z_{ap} - z_{sp} \end{bmatrix} \tag{18}$$

Thus, Communication angles; Azimuth, Elevation, Theta and phi (depicted in the Fig. 1) and range of radio link (distance between satellite and earth stations) have been calculated. Range of the radio link depicted in the Fig. 2 and angles versus time were plotted in the Fig. 3 and Fig. 4.

To determine the instantaneous gains of telemetry transmitter and receiver antennas, instantaneous values of communicative angels should be calculated. With the respect to the 2-D table of telemetry transmit antennas gain and using

communicative angle θ and φ, instantaneous transmit antenna gain is achieved.

In this research, it has been assumed that two source-point transmit antennas has been installed on the satellite in the 10λ distance from each other.

So, with the help of the equation (19), we can calculate the antenna of the transmitter electric field at receiver antenna location.

$$h_{1,2}(\theta,\varphi) = f_{1,2}(\theta,\varphi)\cdot\exp\left[jk\begin{pmatrix} x_{1,2}\sin\theta\cos\varphi + y_{1,2}\sin\theta\sin\varphi + \\ z_{1,2}\cos\theta \end{pmatrix}\right] \quad (19)$$

Where $h_{1,2}(\theta,\varphi)$ is the electric field induced by transmitting antennas at each receiver antenna location, $f_{1,2}(\theta,\varphi)$ is the field radiation pattern, $k = 2\pi/\lambda$ and λ is free space wavelength.

The 2-D table contains antenna gain in each θ and φ angles that is obtained with the direct measuring of antenna gain in the chamber room or analyze antenna theory equations [8, 9]. Based on previous assumption, calculating field radiation pattern and using communicative angle, $G_t(\theta,\varphi)$ is obtained [10, 11];

Fig. 5 depicts resulting pattern from (19) for two transmit antenna in $\theta = 90^\circ$.

III. Calculating Signal to Noise Ratio (SNR)

The transmitter system installed on the satellite would connect directly to the ground receiving station to calculate signal strength at the input of telemetry receiver and also for the mapping of the communicative angles (obtained from the equations in space) to space environment. The following equation is used to calculate the received power of telemetry receiver [12].

$$P_{in} = \frac{P_t\cdot G_t(\theta,\varphi)\cdot f_t(\theta,\varphi)\cdot S_{ef}\cdot L_T}{4\pi R^2} \quad (20)$$

Where, P_{in} is the received power, P_t is the transmitter power, G_t is the transmit antenna gain, f_t is the polarization loss coefficient, S_{ef} is the affective surface of receive antenna, L_T is the total diffuse loss and R is the distance between the receive and the transmit antennas. The value of storing energy in receiver in decibel is given by;

$$S = 10\cdot\log\frac{P_{in}}{P_o} \quad (21)$$

Where, P_o is the sensitivity of the receiver. In the major topics of communication, received SNR is a good indicator for evaluating the radio link. The instantaneous value of this parameter could be used to simulate the instantaneous environment publication [13]. Signal-to-noise ratio is obtained as follow;

$$SNR = \frac{S}{N_0} \quad (22)$$

To calculate the SNR from aforementioned equations, the simulation is accomplished with the parameters as listed in the Table 1.

Table 1
Chosen values of parameters

Parameters	Chosen values
Power of additive Gaussian white noise	-130 dB
Carrier frequency of transmitter	460 MHz
Total diffuse losses	-6 dB
The transmitter power	10 W
The polarization loss coefficient	0.5
Receiver sensitivity	-95 dBm

IV. Simulation Of Radio Link

Channel model for the performance evaluation of modulation method, and channel coding techniques are very important. Channel models are usually classified into two categories; narrowband and wideband. Narrowband channels, for situations where the signal bandwidth is much less than coherent bandwidth in multi-path fading processes, are useful. Rayleigh channels used for the urban cellular channels, Rice channels used in the satellite mobile channels and narrowband channels useful for the aerospace telemetry are as examples for fading narrowband channel models.

The satellite link has been mainly affected by the shadowing in the small elevation angle, no line of sight condition occurs. So, power density function of signal amplitude was Rayleigh distributed. In the larger elevation angle, if direct signal component existed (line of sight condition) the pdf of signal amplitude would be modeled by Rician distribution. The Channel model used in this study for the wideband telemetry link was a multipath channel model with additive white Gaussian noise (AWGN).

Due to the existence or the lack of direct sight component, fading amplitude could be modelled with the distribution of Rician or a Rayleigh. If multi-path reflective paths were large and there was no direct line of sight, fading would be Rayleigh distributed [14]. If the dominant LOS path also existed, the fading would be Rician. Best and worst fading Rician channels would be described by the factor K. If a factor K was zero, Channel would be Rayleigh in the absence of a direct line of sight condition. If a factor K was infinite channel would be Gaussian with strong direct line of sight. So, as a special case of Rician fading channels with K = 0, Rayleigh fading channel was considered. The Rician PDF would be shown as follow [14]:

$$f_{rice}(r) = \frac{r}{\sigma_0^2}\exp\left[-\left(r^2+\beta^2\right)/2\sigma_0^2\right]I_0\left[\frac{r\beta}{\sigma_0^2}\right], \qquad r \ge 0$$

$$k = \beta^2/2\sigma_0^2 \quad (23)$$

Where $I_0[0]$ was the zero-order modified first kind-Bessel functions. Now, if there was no line of sight propagation path, K = 0 and $I_0[0]=1$, the Rayleigh PDF would be shown as follow [14]:

$$f_{rayleigh}(r) = \frac{r}{\sigma_0^2}\exp\left[-r^2/2\sigma_0^2\right], \qquad r \ge 0 \quad (24)$$

Simulation of link was done in 2 cases: first, when no line of sight condition occurred in the small elevation angles, then line of sight condition occurred in the larger elevation angles, for doing this the QPSK modulation with $\pi/4$ phase shift, gray coding and resulting SNR from pervious section has been used [15] and result would be depicted in the Figures 6-9. Rayleigh fading envelope was shown in the Figure 6 and Rice fading envelope was shown in the Figure 7. The simulation result of BER and SER in Rayleigh multipath channel would be shown in the Figure 8 and the simulation result of BER and SER in Rice multipath channel would be shown in the Figure 9. In the Figure 10, BER versus signal to noise ratio in the Rice fading channel for different value of K (for K = 0, 5, 7, 15 dB) would be shown [16 - 18].

To eliminate the effect of Doppler shift, having automatic frequency controller (AFC) in the receiver is necessary. If Doppler shift variation in one period is negligible and the receiver design is correct, carrier frequency offset (CFO) could eliminate the effect of Doppler [19, 20].

Wideband channel models are used in two modes that the signal bandwidth is either in the same order or higher than the coherent bandwidth of fading multi-path process. In this case, the single multi-path reflections, is resolved in the signal bandwidth. The channel has been simulated as a shifted impulses functions with time-varying coefficients that would be able to calculate multi-path characteristics changes. If channel change is slow enough, after a short time interval the channel will be simulated by a LTI system that its base-band impulse response is composed of L diffusion paths, and can be depicted as following form [5];

$$\widetilde{h}(t)=\sum_{k=0}^{L-1}\widetilde{\Gamma}_k \exp\{-j\omega c\widetilde{\tau}_k\}\delta(t-\widetilde{\tau}_k) \tag{25}$$

In trade-off between model accuracy and complexity the number of multi-path reflections (L) used in the model is determined. Generally, in the higher value of L the channel model is more accurate. To represent the multipath interference with reasonable accuracy minimum number of paths, the suitable value for L is equal 3 [5]. The impulse response that is used in aeronautical telemetry channel is depicted as the following form;

$$h(t)=\delta(t)+\Gamma_1\,\delta(t-\tau_1)+\Gamma_2\,\delta(t-\tau_2) \tag{26}$$

Where τ_1 and τ_2 demonstrate delays and two value $\Gamma_1=\Gamma_{1I}+j\,\Gamma_{1Q}$ and $\Gamma_2=\Gamma_{2I}+j\,\Gamma_{2Q}$ demonstrate amplitudes of two multi-path reflections, as introduced in [5]. The received signal is shown by:

$$r(t)=f(t)*h(t)+w(t) \tag{27}$$

$$r(t)=f(t)+\Gamma_1 f(t-\tau_1)+\Gamma_2 f(t-\tau_2)+w(t) \tag{28}$$

Where $w=w_I+j\,w_Q$ demonstrates the additive thermal noise, which is modeled as a complex-valued Gaussian random noise where the real and imaginary part each have been zero mean.

The BER of multipath channel is a function of the multipath parameters Γ_1, τ_1, Γ_2 and τ_2. These parameters are the time variant as the airborne transmitter headway along its flight path. The average values of these parameters have been described in [5], which can be rewritten as follows;

$$|\Gamma_1|=0.85,\quad \tau_1=45ns \tag{29}$$

$$|\Gamma_2|=0.01,\quad \tau_2=155ns \tag{30}$$

So, the channel composed of a line of sight diffusion path and two multi-path reflections. The first reflection has a short delay and large relative amplitude and caused by a specular earth reflection. The second reflection is a weaker reflection.

In the Fig. 11 the simulated bit error probability versus SNR in the input data bit with a bit rate of 10Mbit/s for different values of $|\Gamma_1|$ with phase $\pi/4$, has been plotted. Then, in the Figure 12 the results of simulation modelling to calculate the error rate of bits versus values of $|\Gamma_1|$ for different values of $|\Gamma_1|$ phase in input information bit rate of 10Mbit/s, and SNR=10dB has been plotted and in the Figure 13, could see the simulated channel bit error rate calculated in accordance with the broadband signal to noise in the input bit with different bit rates.

V. Conclusion

According to the importance of telemetry link design, this link should be designed so that against damaging environmental factors not to be impaired. For this purpose, the time variant behavior with the satellite-station radio link is considered and based on the different conditions of propagation link's, there are different modes for the channel. One of the most important parameters in the analysis of the quality of wireless links is SNR, which by its instantaneous calculation, links status can be measured momentarily and BER of the links can be obtained. In this research, BER for QPSK modulation method in frequency selective multi-streaming fading channel is obtained for the space telemetry applications. In the beginning and the end of the satellite observation for the small elevation angles in presence of a powerful multipath reflection the BER with a great error (about 10^{-2}) for $|\Gamma_1|\geq 0.5$ is obtained. But in the greater elevation angles, the reflections have less impacts and BER in the absence of reflections status in Rice channel for K=15dB is calculated about 10^{-7}. By calculating BER momentarily the error could be improved by choosing the type of modulation method, channel accessing method designing and other telecommunication techniques.

References

[1] Marzban S, Mohamedpour K. Calculation of the communication angles between an air vehicle and receiver antenna in aeronautical telemetry. IET Microw Antenna P 2010; 12: 2187-2195.

[2] Jahn A, lutz E. DLR channel measurement programme for low earth orbit satellite systems. In: 1994 Third Annual International Conference on Universal Personal Communications; 27 September – 1 October 1994; San Diego, California, USA: IEEE. pp. 423-429.

[3] Perez-Fontan F, Hovinen V, Schönhuber M, Prieto-Cerdeira R, Teschl F, Kyrolainen J, Valtr P. A wideband directional model for the satellite-

to-indoor propagation channel at S-band. Int J Satell Comm N 2011; 29:23-45.

[4] Parks M, Saunders S, Evans B. Wideband characterisation and modelling of the mobile satellite propagation channel at L- and S-bands. In: 10th International Conference on Antennas and Propagation (Conf. Publ. No. 436); 14-17 April 1997; Edinburgh: IEEE. pp. 39-43.

[5] Rice M, Davis A, Bettweiser C. Wideband Channel Model for Aeronautical Telemetry. IEEE T Aero Elec Sys 2004; 40:57-69.

[6] Rogers R. Applied Mathematics in Integrated Navigation Systems. 3rd ed. USA: American Institute of Aeronautics and Astronautics, 2007.

[7] Vanicek P, Krakiwsky J. Geodesy: The Concepts. 2nd ed. North-Holland, 1986.

[8] Reddemann J. range telemetry evaluation. In: Proceedings of the International Test and Evaluation Association Conference; April 1997; Lancaster, CA, USA: AEA. pp. 51-57.

[9] Pedroza M. Antenna pattern evaluation for link analysis. In: Proceedings of the International Telemetering Conference; October 1996; San Diego, CA, USA: IEEE. pp.158-166.

[10] Balanis. C. A. Antenna theory: analysis and design. 3rd ed. New York NY, USA: Wiley, 2005.

[11] Jensen M, Rice M, Anderson A. Aeronautical telemetry using multiple-antenna transmitters. IEEE T Aero Elec Sys 2007; 43:262-272.

[12] Frank C, Russell J, Robert H. Telemetry Systems engineering. Boston, London: Artech House, 2002.

[13] Proakis J. Digital Communications. 5th ed. New York NY, USA: McGraw-Hill, 2007.

[14] Sklar B. Rayleigh Fading Channels in Mobile Digital Communication Systems partı: Characterization. IEEE Commun Mag 1997; 35:90-100.

[15] Rice M, Dang X. Aeronautical Telemetry using Offset QPSK in Frequency Selective Multipath. IEEE T Aero and Elec Sys 2005; 41:758-766.

[16] Kostov N. Mobile Radio Channels Modeling in MATLAB. Radio Eng 2003; 12: 12-16.

[17] Proakis J, Salehi M. Contemporary Communication Systems Using MATLAB. Boston: PWS publishing company, 1998.

[18] Fischer St, Seeger R, Kammer D. Implementation of a Real-Time Satellite Channel Simulator. In: The 3rd European DSP Education and Research Conference; 20-21 September 2000; Paris, France: ESIEE. pp. 1-5.

[19] Maral G, Bousquet M, Sun Z. Satellite Communications Systems: Systems, Techniques and Technology. 5th ed. New York, NY, USA: Wiley & Sons, 2009.

[20] Saunders R. Antenna and propagation for wireless communication systems. 2nd ed. New York, NY, USA: Wiley & Sons, 2007.

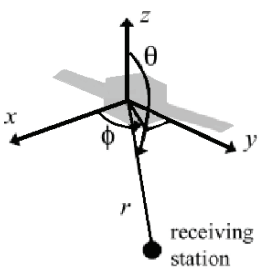

Figure 1: Communication angles between transmit and receive antennas

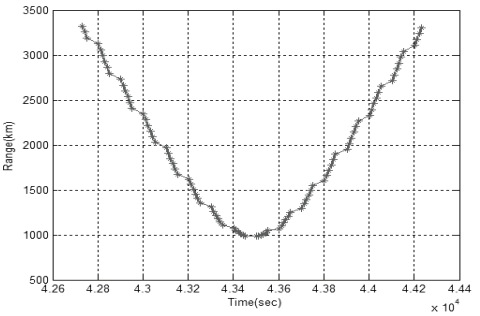

Figure 2: Distance between satellite- earth station versus time

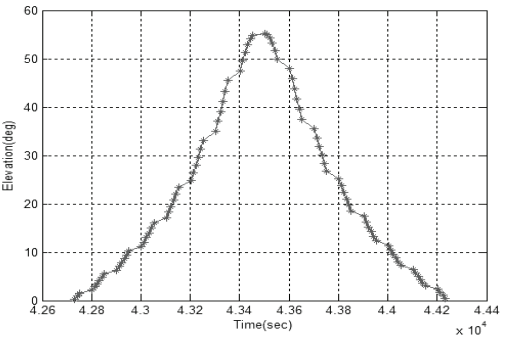

Figure 3: Elevation angle versus time

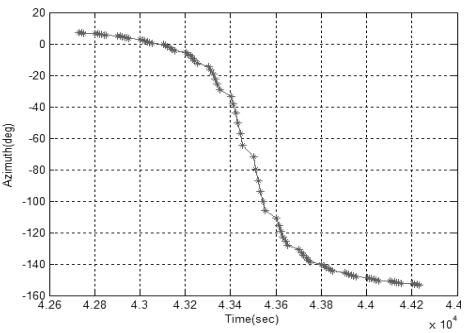

Figure 4: Azimuth angle versus time

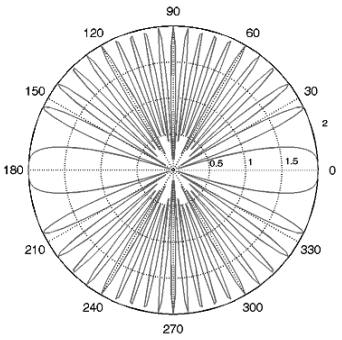

Figure 5: Radiation pattern for 2 antennas on satellite in θ=90° and φ=0~360°

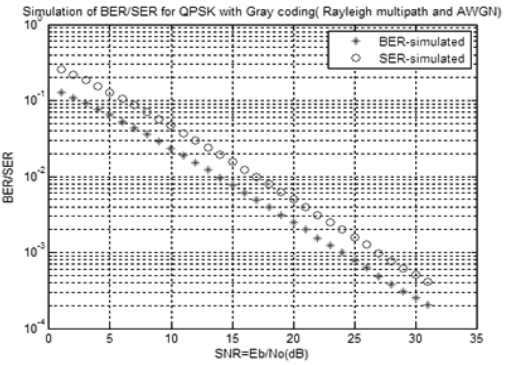

Figure 8: BER and SER of Rayleigh multipath and AWGN

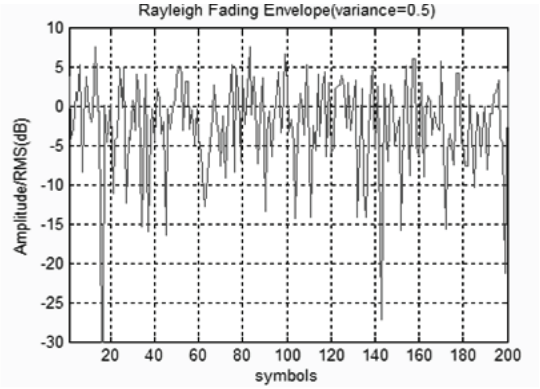

Figure 6: Rayleigh fading envelope

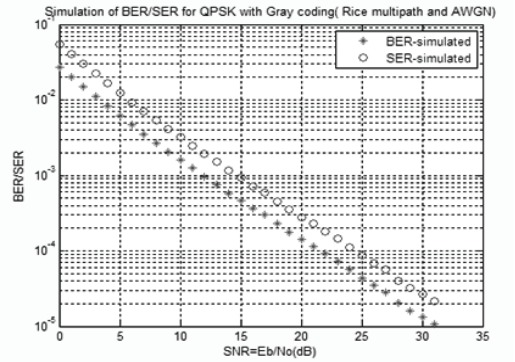

Figure 9: BER and SER for rice multipath and AWGN for K = 7dB

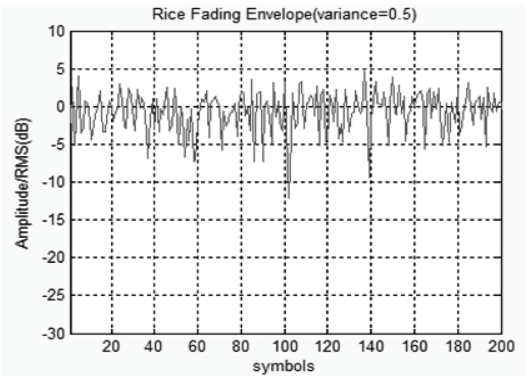

Figure 7: Rice fading envelope for K = 7dB

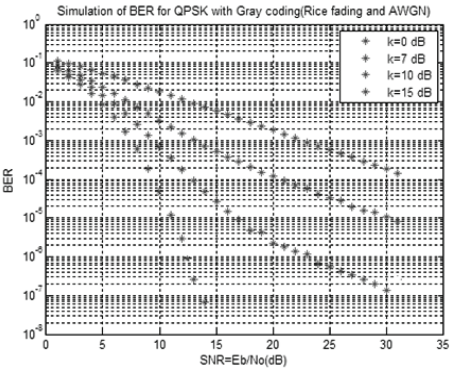

Figure 10: BER versus signal to noise ratio in the Rice fading channel (for K = 0, 5, 7, 15dB)

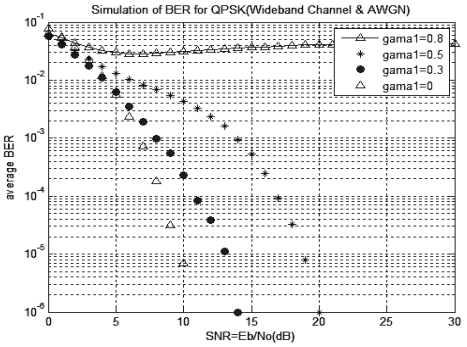

Figure 11: BER versus signal to noise ratio for different values $|\Gamma_1|$ with phase π /4 and bit rate of 10Mbit/s

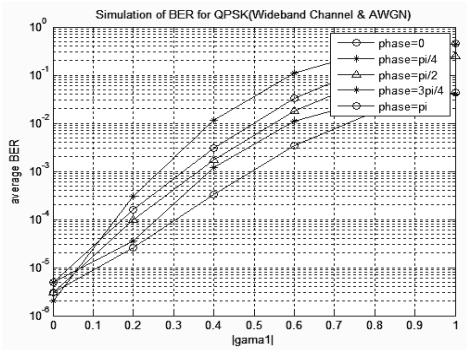

Figure 12: BER versus $|\Gamma_1|$ for different values of Γ_1 phase in bit rate of 10Mbit/s, and SNR =10dB

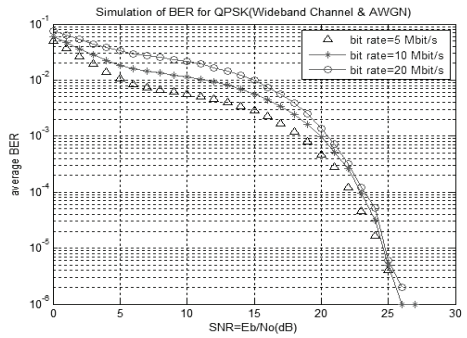

Figure 13: BER versus signal to noise ratio at different bit rate